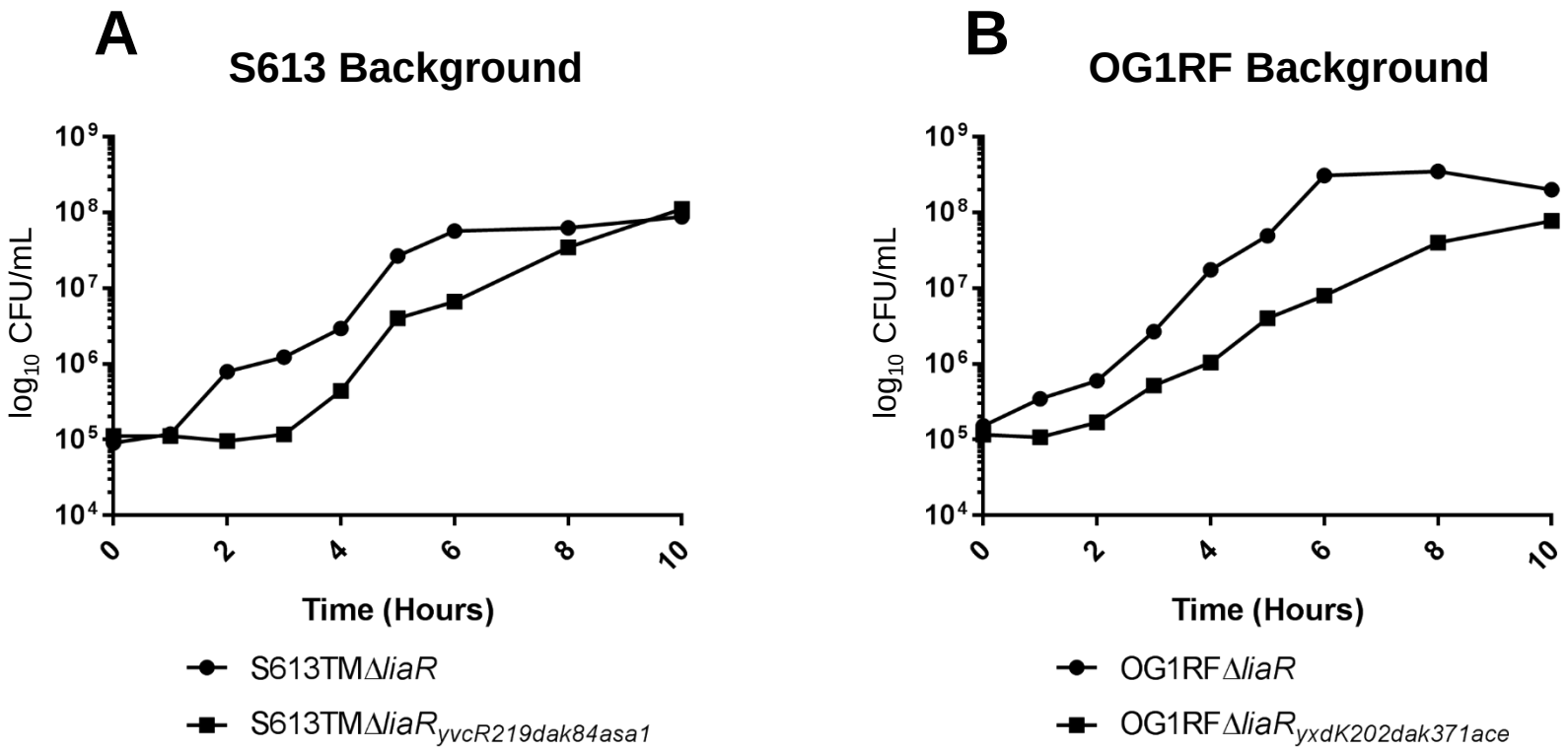


**Supplementary Figure 1. Correlation of $A_{600nm}$ to viable colony forming units.** Growth phenotype of (A) S613TMΔ*liaR* background and (B) OG1RFΔ*liaR* background determined by viable colony forming units (CFU) per milliliter. The *in vitro* generated resistant mutants in both strain backgrounds displayed an increase in the lag phase and slower time to final cell density, consistent with the growth curves generated via measurement of absorbance by automated spectrophotometer.

**S613TMΔ*liaR*$_{yvcR219dak84asa1}$** **OG1RFΔ*liaR*$_{yxdK202dak371ace}$**


**Supplementary Figure 2. Stability of the DAP-R phenotype.** Stability of the DAP-R phenotype of S613TMΔ*liaR*$_{yvcR219dak84asa1}$ and OG1RFΔ*liaR*$_{yxdK202dak371ace}$ was determined by E-test after 7 days of passage in antibiotic free BHI broth. S613TMΔ*liaR*$_{yvcR219dak84asa1}$ retained a resistant phenotype without a change in the MIC. OG1RFΔ*liaR*$_{yxdK202dak371ace}$ displayed a heterogeneous population, with a dual halo indicative of a resistant sub-population.

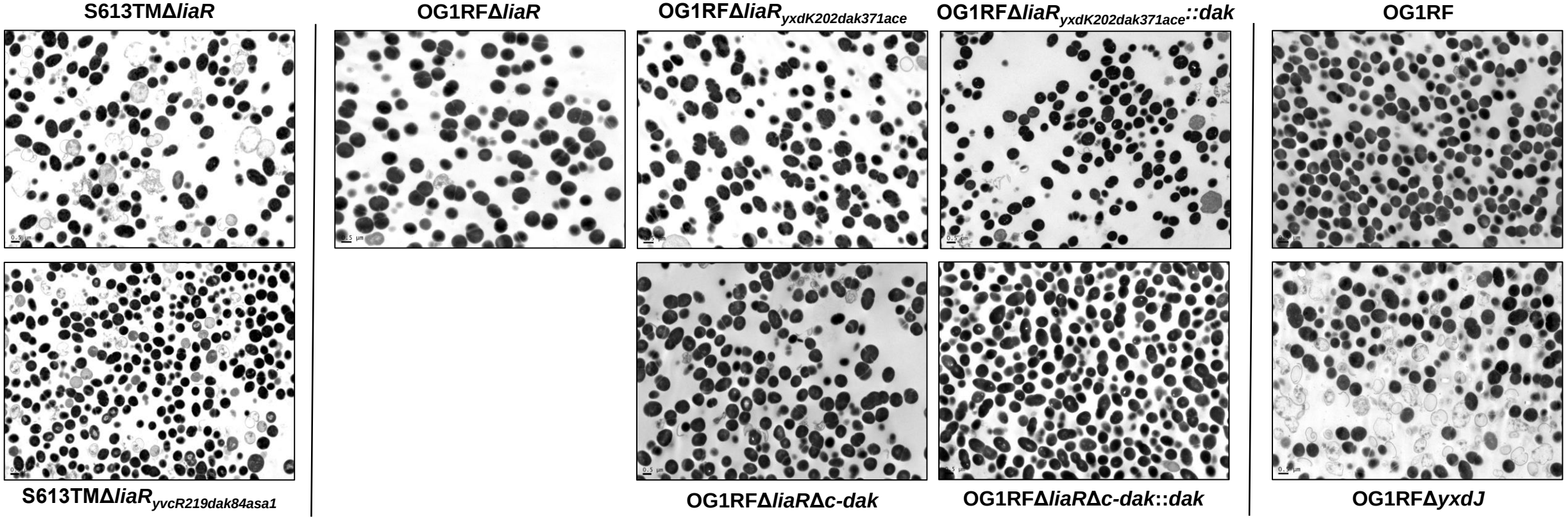


**Supplementary Figure 3. Wide-field TEM for *E. faecalis* strains.** Representative wide field TEM images for each strain at 5,000x magnification. Top row, parent strains. Bottom row, derivative strains. Strains OG1RFΔ*liaR*$_{yxdK202dak371ace}$ and OG1RFΔ*liaR*Δ*c-dak* are notable for cells with abnormal division plane and altered cell morphology.

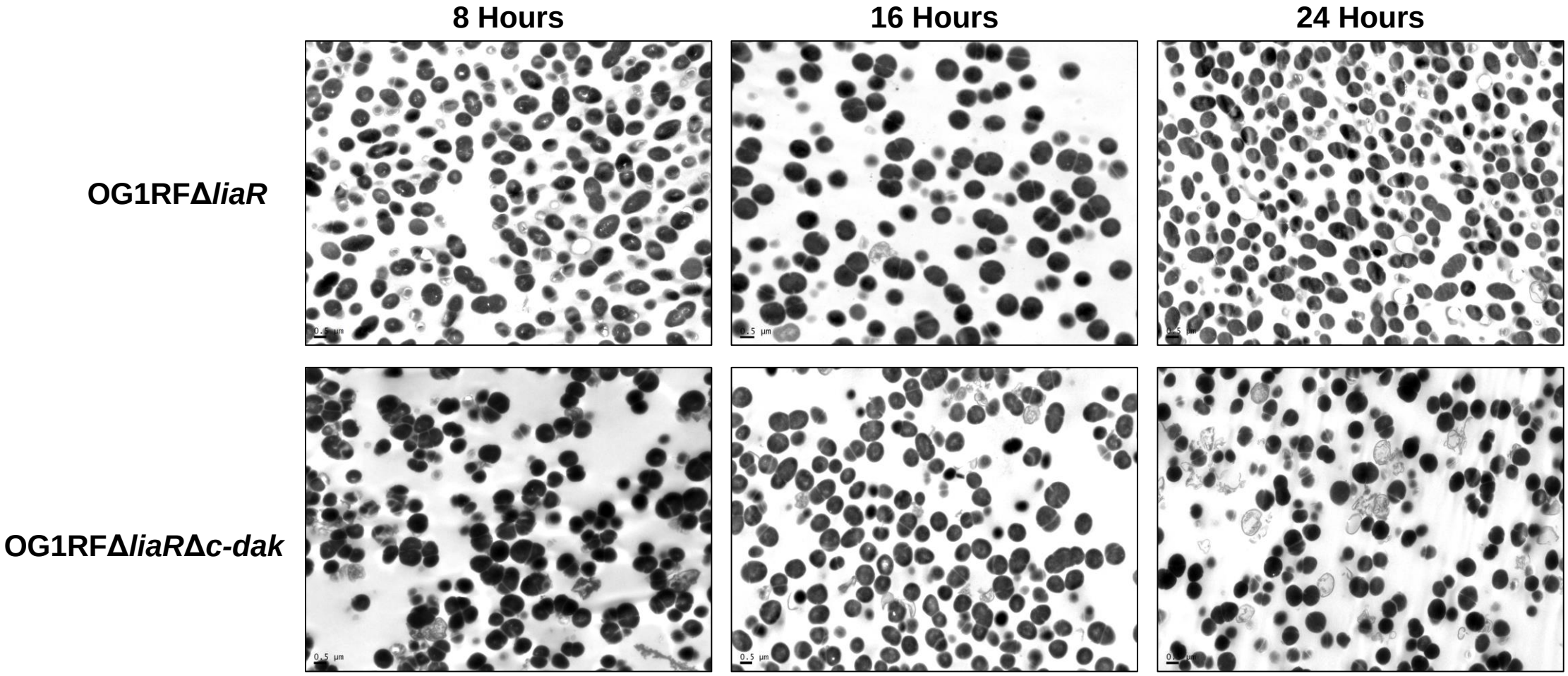


**Supplementary Figure 4. Wide-field TEM for OG1RFΔ*liaR* and OG1RFΔ*liaR*Δ*c-dak* across time points.** Representative wide field TEM images for each strain at 5,000x magnification. Top row, OG1RFΔ*liaR*. Bottom row, OG1RFΔ*liaR*Δ*c-dak*. Changes in cell morphology for OG1RFΔ*liaR*Δ*c-dak* are more pronounced during late-exponential phase growth (8 hours).

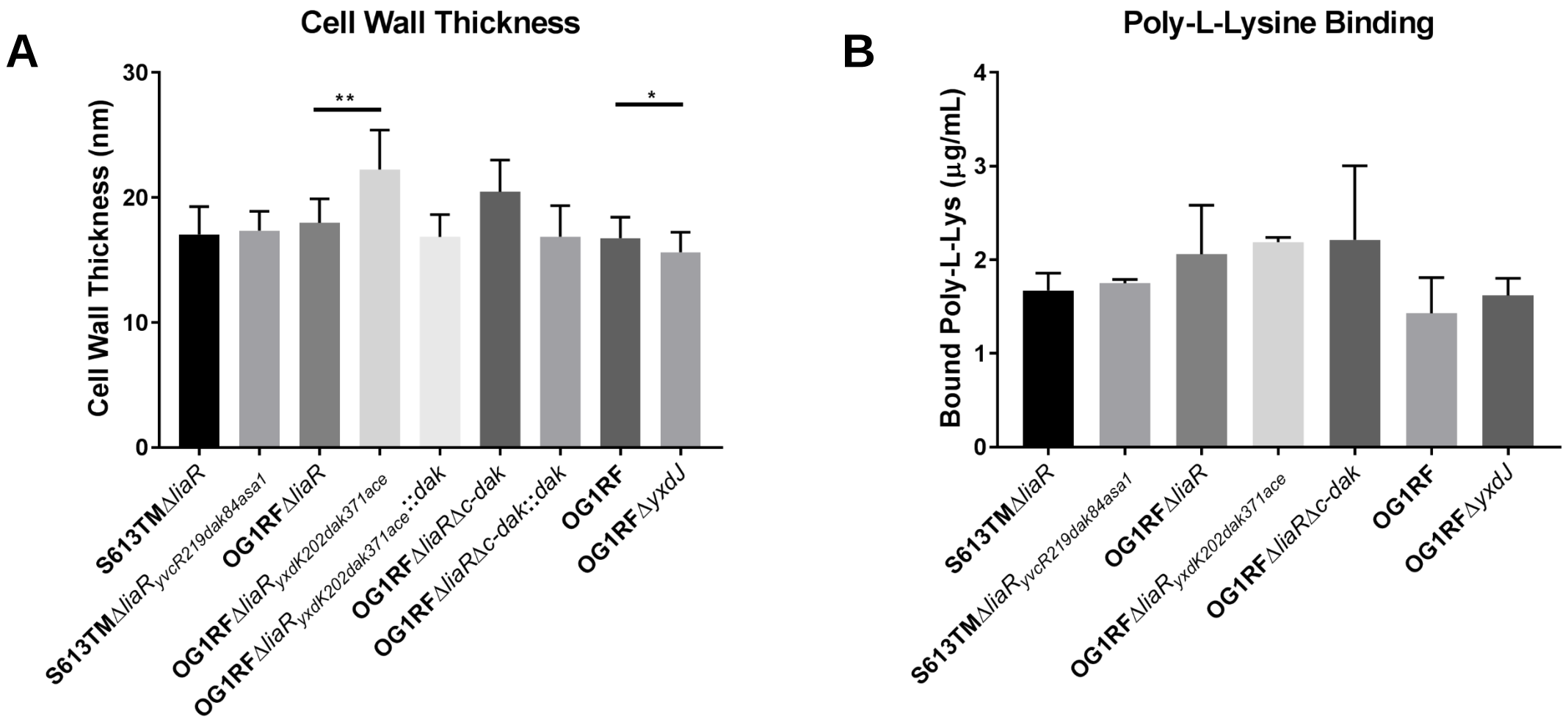


**Supplementary Figure 5. Cell wall thickness and cell surface charge for *E. faecalis strains.*** A) Cell wall thickness based on measurements from TEM images (from the outer edge of the cell membrane to the outside of the cell wall, minimum 25 cells). **, $p<0.01$; *, $p<0.05$; ns, non-significant. B) Cell surface charge as determined by Pol-L-Lysine binding (n=3 independent runs, each in technical triplicate). Since Poly-L-Lysine is a positively charged molecule, decreased binding indicates an increase in overall positive cell surface charge. There were no significant differences between the strains.

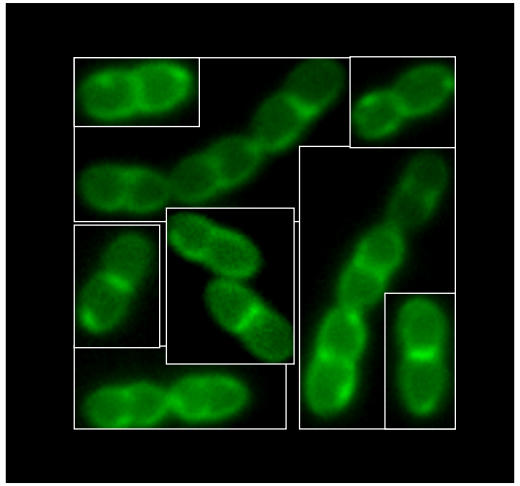

S613TMΔ*liaR*

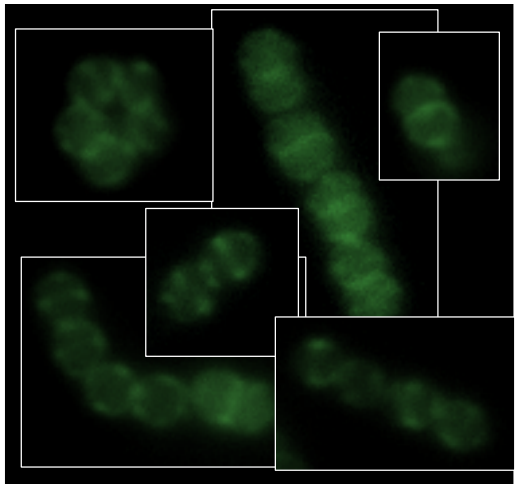

S613TMΔ*liaR*$_{yvcR219dak84asa1}$

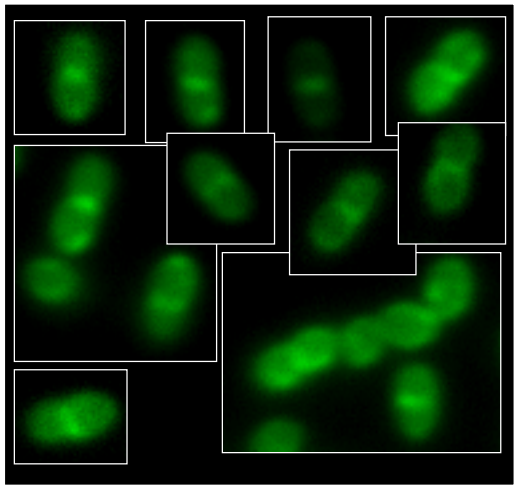

OG1RF

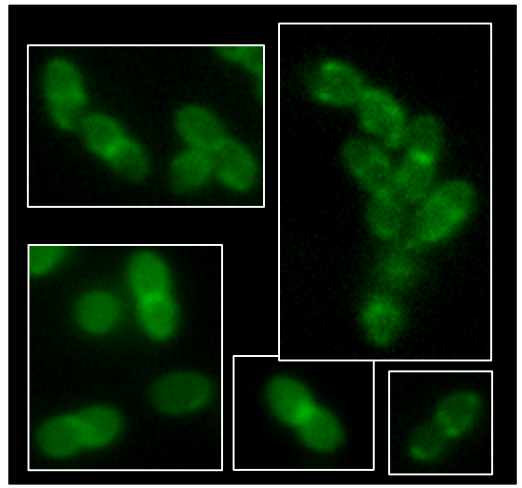

OG1RFΔ*yxdJ*

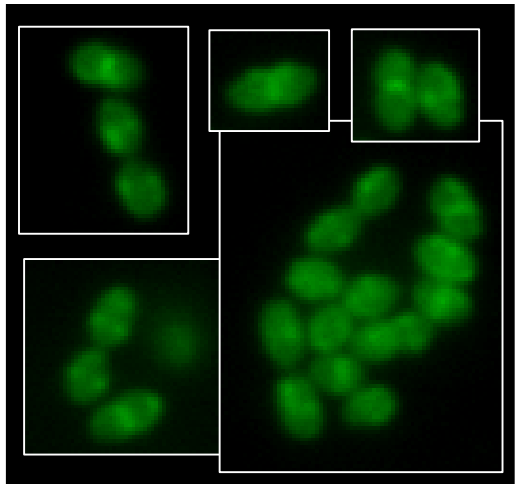

OG1RFΔ*liaR*

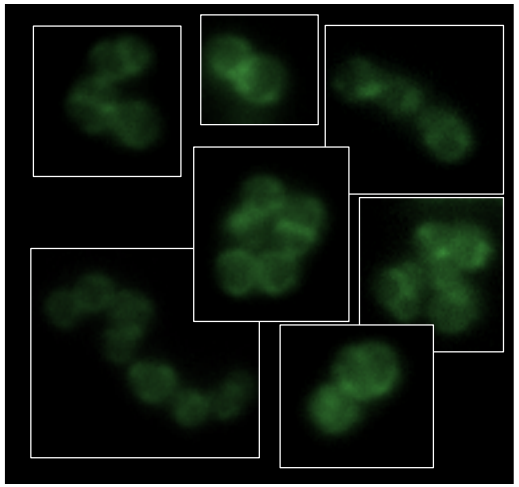

OG1RFΔ*liaR*$_{yxdK202dak371ace}$

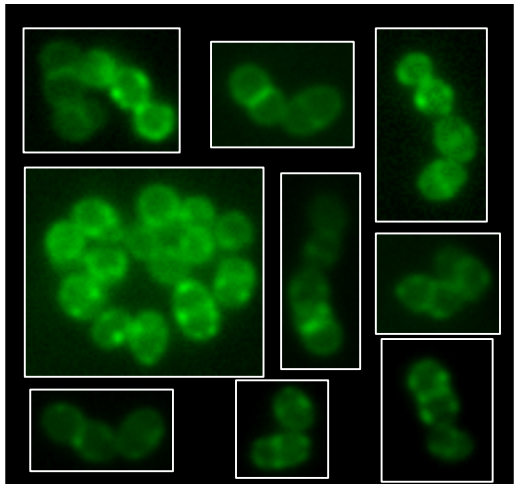

OG1RFΔ*liaR*Δ*c-dak*

**Supplementary Figure 6. *E. faecalis* strains stained with *N*-nonyl Acridine orange (NAO).** Representative NAO stained cells selected from multiple fields of view. NAO staining was noted primarily in septal areas without redistribution. OG1RFΔ*liaR*$_{yxdK202dak371ace}$ and OG1RFΔ*liaR*Δ*c-dak* displayed an increased tendency to clump with varying cell shapes and sizes consistent with TEM observations.

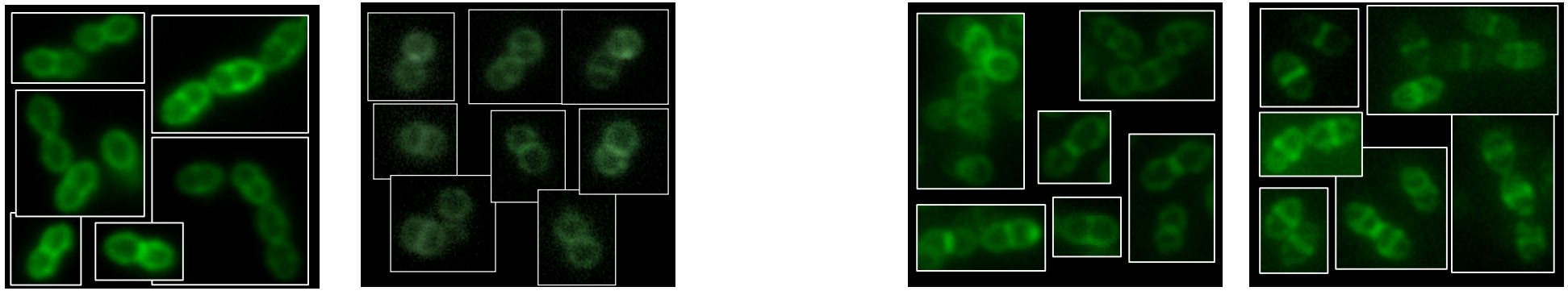


**Supplementary Figure 7. *E. faecalis* strains stained with BODIPY-DAP.** Representative cells from strains stained with BODIPY-DAP selected from multiple fields of view. Septal staining is evident in all strains without diversion of the fluorescent DAP molecule. OG1RFΔ*liaR*$_{yxdK202dak371ace}$ and OG1RFΔ*liaR*Δ*c-dak* displayed altered cell morphology with multiple septal events per cell consistent with TEM imaging.

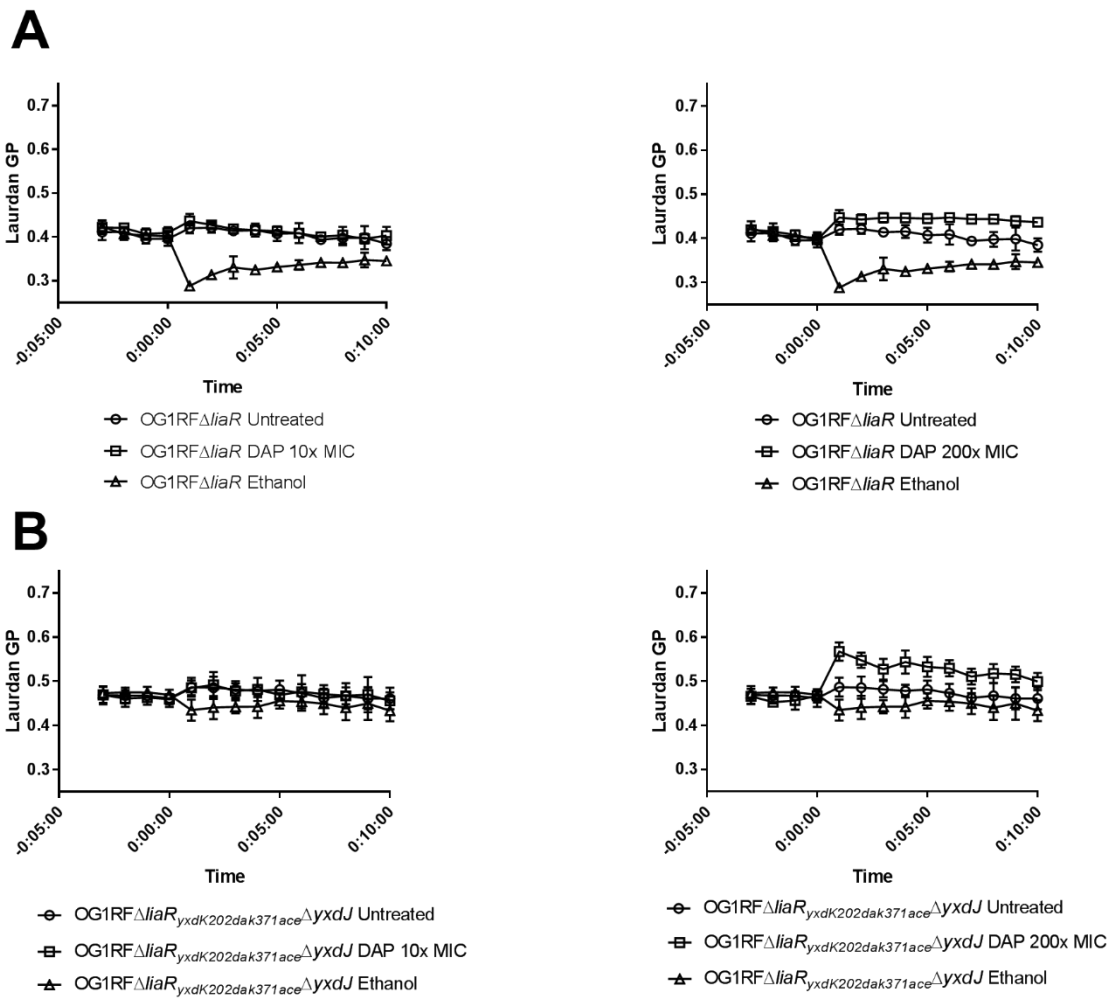


**Supplementary Figure 8. DAP associated changes in membrane fluidity vary with DAP concentration.** Laurdan generalized polarization spectroscopy of A) OG1RFΔ*liaR* (DAP MIC 0.047 µg/mL) and *B)* OG1RFΔ*liaR*$_{yxdK202dak371ace}$Δ*yxdJ* (DAP MIC 0.094 µg/mL) at 10x (left panel) and 200x MIC (right panel). The degree of observed membrane rigidity correlates with absolute DAP concentration, with increased rigidity seen at 200x MIC (9.4 and 18.8 µg/mL , respectively); however, at 10x MIC (0.47 and 0.94 µg/mL, respectively) no apparent shift in rigidity is seen.

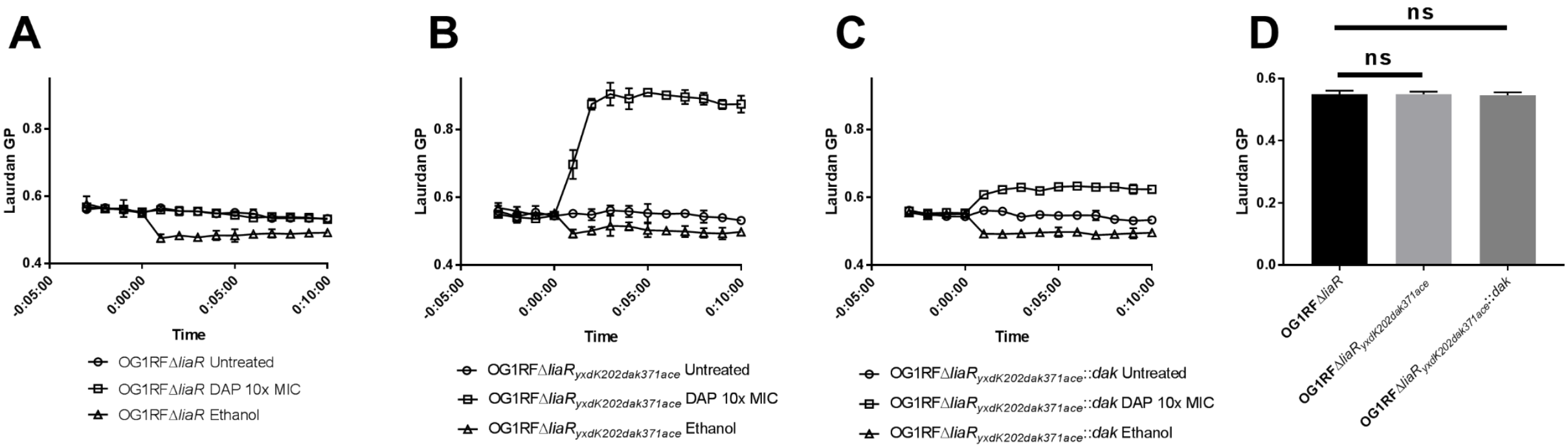


**Supplementary Figure 9. Dak associated changes in membrane fluidity are growth phase dependent.** Laurdan generalized polarization spectroscopy of A) OG1RFΔ*liaR,* B) OG1RFΔ$liaR_{yxdK202dak371ace}$ and C) OG1RFΔ$liaR_{yxdK202dak371ace}$::*dak* from cells grown to stationary phase. As compared to cells in exponential phase (see main text Figure 4), cell membranes of cells in stationary phase were more rigid, and no difference was seen between OG1RFΔ*liaR,* the DAP-R OG1RFΔ$liaR_{yxdK202dak371ace}$ or the *dak* complemented strain (D). Representative results of two independent assays for each strain performed on different days. ns, non-significant.